Dynamics of Axial Segregation and Coarsening of Dry Granular Materials and Slurries in Circular and Square Tubes

S. J. Fiedor and J. M. Ottino
Department of Chemical Engineering, Northwestern University, Evanston, Illinois 60208, USA
(Received 14 May 2003; published 10 December 2003)

We study segregation and coarsening dynamics of dry granular materials and slurries in tubes with circular and square cross sections. Space-time plots show key differences between the four cases, including band splitting and wave formation, depending upon the rotational speed. However, the fraction of the surface occupied by bands of small-rich particles is nearly constant in all experiments, leading to quasi-1D behavior, and the rate of coarsening, when it occurs, is logarithmic in all cases. Coarsening rates are very similar except in the case with the longest development time.

DOI: 10.1103/PhysRevLett.91.244301 PACS numbers: 45.70.Mg, 05.65.+b, 45.70.Qj

Introduction.—Axial segregation of granular materials has become a prototypical problem in pattern formation. Rotated cylindrical tumblers filled with binary mixtures lead to the formation of axial alternating bands of large/small (S systems) or dense/less-dense materials (D systems) [1,2]. A few facts are well established for half full containers; upon rotation, particles first separate radially in the plane perpendicular to the axis of rotation, forming a classical radial segregation pattern in the circle [3], and two rotating lobes in the cases of squares [4] (see Fig. 1). This process occurs very quickly, within a single rotation. Within the next $O(10^1–10^2)$ rotations, the particles separate further into bands of seemingly monodisperse regions and a complex dynamics of bands merging may ensue. Little is known about the dynamics of coarsening of axially segregated systems over long periods of time. Quantitative analysis is still limited; granular dynamics theory is still insufficiently developed and experiments have covered only a limited region of the parameter space. Consider a few key experiments.

Nakagawa studied long-term behavior [5]. He found that a system consisting of two different sized particles might contain as few as three bands. Other investigators focused on the reversibility of the segregation [6,7]. Hill *et al.* also studied the interior structure of axial segregation using magnetic resonance imaging (MRI) and the evolution of band merging using surface images and MRI [8,9]. MRI showed that the bands of larger particles still had cores of smaller particles. The larger particles form rings around the radial core of the smaller particles.

Axial segregation was recently discovered in slurries [10], that is when a liquid replaces air as the interstitial fluid. The advantage of using a liquid is the investigation of the internal structure of the system via index matching and the ability to control particle interactions [11]. The relative effect of the lubrication forces to the collisional forces is given by the Bagnold number ($B = \rho d\dot{\gamma}\epsilon/\mu$), while the Leighton number [$L = \mu\dot{\gamma}/\epsilon g(\rho - \rho_{\mathrm{fluid}})$] gives the relative effect of the lubrication force to the frictional forces (here d is the particle diameter, $\dot{\gamma}$ is the shear rate, ϵ is the length scale of the roughness, ρ is the particle density, ρ_{fluid} is the fluid density, μ is the fluid viscosity, and g is the gravity.) In the systems considered here, B ranges from $O(10^2–10^3)$ for dry systems and $O(10^{-2}–10^{-1})$ for slurries. L ranges from $O(10^{-3})$ for dry systems and $O(10^{-2}–10^{-1})$ for slurries.

Experimental results.—We consider four different types of experiments: dry granular materials and slurries in circular and square acrylic tumblers. The circular tumbler has an inner diameter of 2.5 in. (63.5 mm) and the square tumbler has an inner side length of 2.25 in. (57.15 mm). Both are 30 in. (760 mm) long. Experiments consist of rotating two different sized glass beads (density 2.5 g/cm^3) at various rotation rates. The smaller beads are 300 μm in diameter and dark in color, while the larger beads are either 900 μm or 1200 μm in diameter and clear. The first set of experiments uses 900 μm beads; the second 1200 μm beads. The degree of filling is 1/2 and kept constant in all experiments. In the slurry experiments, water fills the remaining volume of the tumblers completely. A trace of soap is also added to reduce the surface tension and minimize the amount of trapped air bubbles. Humidity was not monitored in the dry experiments, but clumping or static effects were not encountered.

A Compumotor stepper motor is used to rotate the tumblers and a Kodak Megapixel 1.4i digital camera is

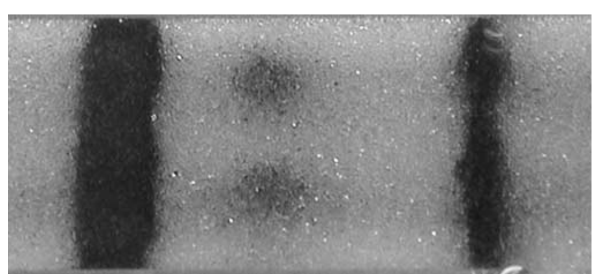

FIG. 1. Bottom view of bands at three different stages of formation in a square tumbler. Complete band (left), partial band (right), and lobes growing in the core region (center).

used to image the experiments. The camera is positioned at a distance far enough away (~4 m) to ensure that the entire side of the tube is captured in each image. The maximum camera width resolution is 1316 pixels resulting in approximately 580 μm/pixel, or roughly two small particles per pixel. The motor and the digital camera are controlled by sending commands from a single Visual C++ program. By doing this, the tumbler position can be monitored and digital images could be captured at accurate times or positions for any number of rotations.

The evolution of the segregation process is presented in terms of space-time plots (Fig. 2). The plots are constructed in the following way. Images taken at each rotation are cropped to the length of the tumbler and a height of one pixel. The slice is taken just below the surface to ensure the darker core color does not affect the surface color. The cropped images are then stacked on top of each other to create a spatiotemporal series. A Gaussian blur is then used on the spatiotemporal images to eliminate any noise. The vertical radius of the Gaussian blur was twice that of the horizontal radius in order to reduce the noise in time more than the noise in space. The spatiotemporal images are then thresholded and the pixel values read and written to a file using MATLAB.

The space-time plots can be used to obtain a variety of data, such as the number of bands, average width, and variance as a function of time or rotations. In particular, they can be used to obtain the fraction of the surface or visible area occupied by the smaller (darker) beads. Since the time scale associated with band motion is much longer than the time scale of one revolution, a row of pixels is sufficient to represent the total area of the bands at a particular time. The total number of pixels associated with smaller particles yields the fractional area of bands consisting of smaller particles.

Results and discussion.—Consider first a few general observations and definitions of terminology. All experiments are run in the continuous flow regime. The segregation, when viewed from the side, has a shish kebab or abacuslike architecture with a domain of small particles being pierced by a rod spanning the length of the tube. (The structure can be clearly visualized by index matching experiments [10]; however, it is also visible under suitable illumination when using clear beads.) The large transparent particles are effectively segregated, forming disconnected rings. On the other hand, the black smaller particles interact directly via the radial core. The initial formation of the radial core in square geometries is very much like what is seen in quasi-2D experiments: First spots appear and then complete bands (see Fig. 1).

We label the cases as geometry-system: that is, circle-dry, circle-slurry, square-dry, and square-slurry. We report comparisons across all cases for 4 rpm; the experiments involving dry systems are run under faster conditions (10, 15, 20, and 25 rpm) than the slurry systems (3, 5, 7, and 9 rpm). The rpm studied span the range from the slowest speed beyond the avalanching regime to the fastest speed before the interface becomes noticeably curved. It is then apparent that the dry and slurry cases require different RPM intervals. Here we present a subset of all the rpm investigated.

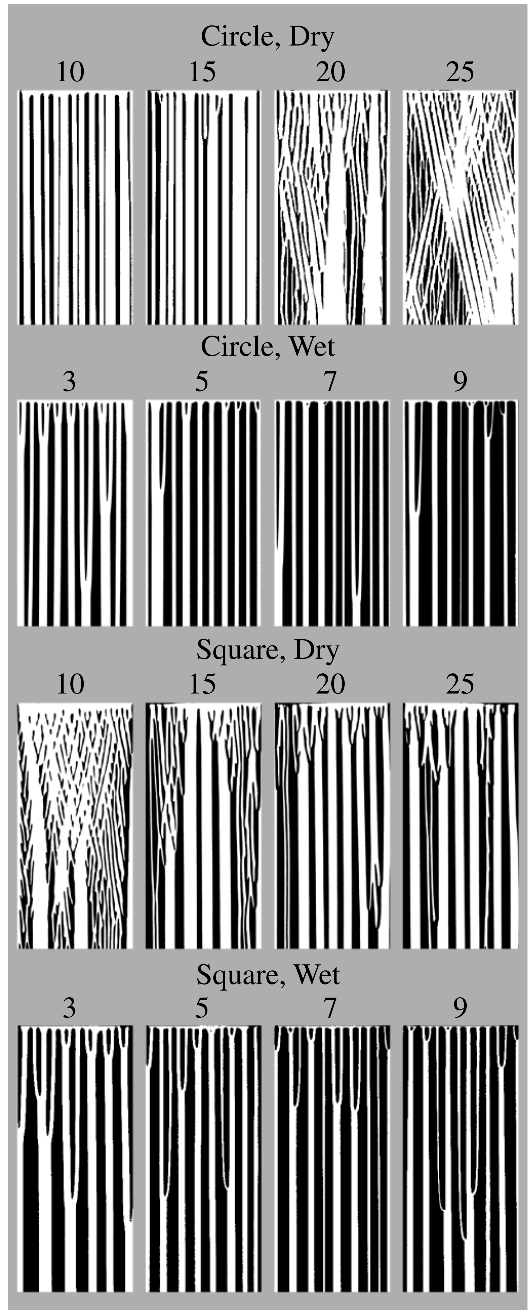

FIG. 2. Representative experimental space-time plots at various rotation rates for the four studied systems. All experiments pictured were run for 2500 rotations. Dry experiments were run at 5, 10, 15, 20, and 25 rpm, and wet were run at 3, 5, 7, and 9 rpm. In every figure the top corresponds to the initial condition.

Figure 2 shows the main results of the four cases. The top row corresponds to the circle-dry case, the most studied in the literature. However, an exploration of the rpm parameter space reveals new aspects. At the slowest possible speed the system never settles down in a segregating regime within 2500 revolutions. At 10 rpm, segregation is extremely fast and no coarsening occurs during the entire duration of the experiment; at 15 rpm, the second case from the left (and in fact the entire second row of Fig. 2) corresponds to what we call standard

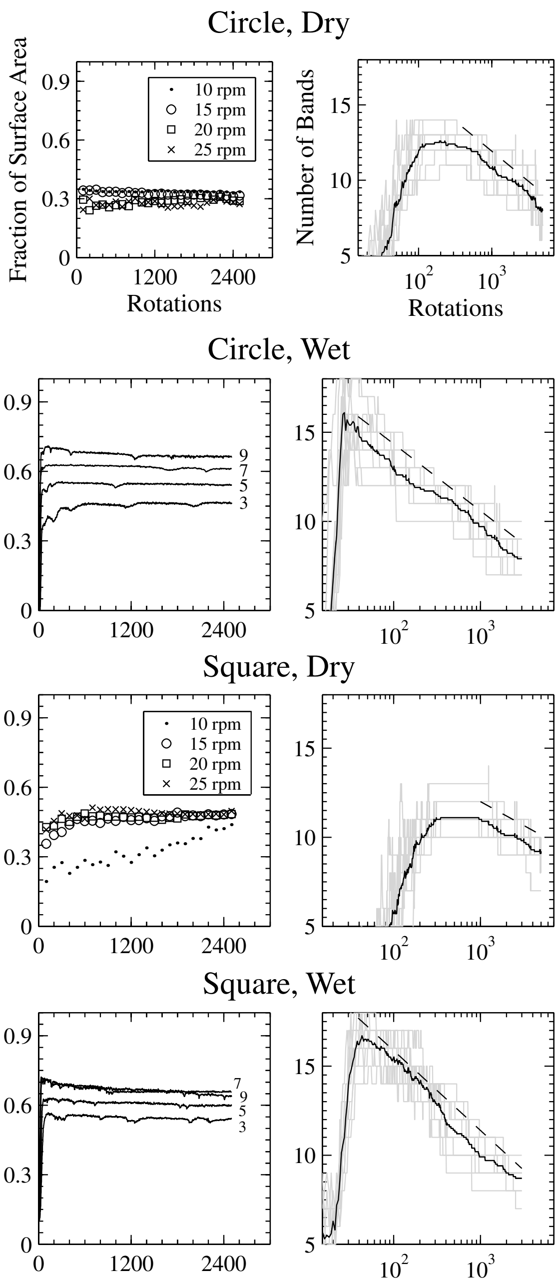

FIG. 3. Plots of the number of bands and fraction of surface area for the four systems. The column on the left shows the area fraction of the darker beads at various rotation rates. The column on the right shows the evolution of the number of bands. The gray lines correspond to ten different realizations of the experiment. The dashed line shows the slope of the best fit.

coarsening. That is, there is no evidence of waves, fingering, and no other bands are formed other than the initial bands [those formed within $O(200)$ rotations]. At 20 rpm, the behavior is considerably more complex and, at 25 rpm, we observe the presence of traveling waves similar to those reported by Choo *et al.* [12]. The second row corresponds to the circle-slurry case. It is apparent that the addition of a fluid leads to standard coarsening at all speeds with the thickness of the bands of smaller size materials increasing with increasing speed. The case of square-dry (third row) shows band splitting at all speeds with the most interesting dynamics occurring at low speeds; the higher speeds involve a competition between coarsening and splitting. The square-slurry (fourth row) case shows standard coarsening at all rpm.

A key result is the constancy of the fractional area of the bands (Fig. 3, left column). In the circle-dry case, the amount of visible area asymptotes quickly and remains constant with all speeds, clustered between 0.25 and 0.37 with the maximum percentage corresponding at the lowest speed. The circle-slurry cases asymptotes, though less quickly, and the maximum percentage corresponds to the highest speed. The maximum value is about 0.70. The square-dry case asymptotes very slowly, especially at low speeds, and eventually all curves converge to a value in the neighborhood of 0.50. The square-slurry is the only case that overshoots (slightly) and quickly asymptotes with the maximum percentage occurring at the highest speed as in the previous slurry case. The visible area is constant with time in all cases considered indicating that the core structure remains unchanged. Mixing of large and small particles occurs, especially in the case of slurries where the amount of dark domains approaches 0.70. Visual inspection shows that the bands of larger particles are nearly pure (they are transparent). This indicates that the small particles are mixed with the large particles.

It is evident that not all speeds lead to coarsening. In order to study the long time behavior of coarsening, we selected specific speeds and repeated each experiment ten times. The dry case was run at 12 rpm (not shown in Fig. 2) for 5000 revolutions and the slurry case at 5 rpm for 3000 revolutions. The size of the larger, clear beads was 1200 μm to ensure standard coarsening; all other parameters remained the same. The faint grey lines in Fig. 3 indicate the evolution of the number of bands in the ten runs. In all cases there is a development time before all the bands form (upward section of the curves). In each experiment, the individual bands do not reach the surface at the same time. In the dry experiments, the first bands to form are at the ends, and over time other bands reach the surface throughout the tumbler seemingly randomly. Also, the bands at the ends always involve the larger particles. At first, this might lead to the conclusion that the shear at the ends induces axial banding throughout the tumbler. However, numerous experiments in our laboratory at slower rotation rates show that bands do emerge in the middle of tumblers before the end effects can propagate inward. In the case of slurries, bands also form randomly throughout the tumbler, but substantially faster (see Fig. 3, right column).

The average (less the initial band formation) is fitted to a log curve. The right column of Fig. 3 shows the experimental data, the average curve, and the fitted curve on a single plot. For clarity, the slope is plotted separate from the average curve. It is apparent that, when coarsening begins, the number of bands follows a logarithmic decay, $-k \ln(n)$, where n is the number of revolutions. The rate of decay in both of the circular cases is very similar to the slope k, being 1.740 ± 0.05 (circle-dry) and 1.630 ± 0.07 (circle-slurry). The slopes in the square cases are 1.170 ± 0.13 (square-dry) and 1.940 ± 0.04 (square-slurry). The standard deviation in the fitting was determined using the set of nine exponents calculated by eliminating one out of the ten repeated runs. Our systems are manifestly 3D. However, the conservation of species shown in the left column of Fig. 3 suggests that the process can be viewed as 1D. A $\ln(t)$ behavior arises in theoretical models of 1D coarsening [13] and in some theoretical models of 3D systems [14]. It is also important to note that a logarithmic decay is predicted by the theory of Aranson and Tsimring [15] and Aranson *et al.* [16] developed for axial segregation of granular materials. We should point, however, that there is still also considerable debate as to the equations governing granular dynamics, for example, the effects of the subsurface flow need to be taken into account [17]. In general, the number of experiments of coarsening in 1D is limited (except for those involving defects) and certainly much smaller than those in 2D and 3D [18]. The reason is that, if one creates a system with stripes of materials of various widths, say, on a surface, these stripes are susceptible to a Rayleigh instability. Thus, rather than coarsening (by increasing the width of the stripes) the stripes break up into droplets. Thus, most of the studies of coarsening of materials in 1D have been primarily theoretical or have focused on defects. The present results pose a challenge to the theoretical community.

The main limitation of these studies is that they report only what is visible at the surface of the tumbler. It is also worth pointing out that we expect the results in the case of the square tumbler to depend significantly on the degree of filling, as shown by Hill *et al.* [6,17]. The range of rotation rates used in slurry experiments is smaller than those of the dry experiment. The slurry systems used in this study are restricted due to a noticeably curved interface and mixing at faster rotation rates. Thus, nonstandard coarsening in slurries may not be ruled out; the parameter space studied is small. The concentration of smaller particles could be reduced to expand the range of rpm. This may reveal where waves and fingering may exist. The logarithmic decay regimes are well defined in all experiments, the weakest case being the dry square container. In all experiments, the initial number of bands is about 15 and the final number of bands is about 5. Thus, to increase the range in the number of bands formed would require longer tubes. Also, there are transitions between regimes, which define the operability region. No attempt was made to precisely identify the rpm of these transitions.

The slurry experiments shown in Figs. 2 and 3 were conducted using water as the interstitial fluid. Using a fluid with different properties changes the magnitude of the forces involved. Results in our laboratory show that increasing viscosity results in an increase in the fraction of surface area of small-rich particles. However, bands do start to become unstable and "wavy" at higher viscosities when the bands composed of larger particles fall below a critical thickness. These issues deserve full attention and will be reported in future work.

This research was supported by DOE, Office of Basic Energy Sciences. We would like to thank Peter Vorhees and Stephen Watson for useful discussions.

[1] J. Duran, *Sands, Powders, and Grains* (Springer, New York, 2000).
[2] G. H. Ristow, *Pattern Formation in Granular Materials* (Springer-Verlag, Berlin, 2000).
[3] D.V. Khakhar, J. J. McCarthy, and J. M. Ottino, Phys. Fluids **9**, 3600 (1997).
[4] K. M. Hill, D.V. Khakhar, J. F. Gilchrist, J. J. McCarthy, and J. Ottino, Proc. Natl. Acad. Sci. U.S.A. **96**, 11701 (1999).
[5] M. Nakagawa, Chem. Eng. Sci. **49**, 2540 (1994).
[6] K. M. Hill and J. Kakalios, Phys. Rev. E **49**, R3610 (1994).
[7] K. M. Hill and J. Kakalios, Phys. Rev. E **52**, 4393 (1995).
[8] K. M. Hill, A. Caprihan, and J. Kakalios, Phys. Rev. Lett. **78**, 50 (1997).
[9] K. M. Hill, A. Caprihan, and J. Kakalios, Phys. Rev. E **56**, 4386 (1997).
[10] N. Jain, DV. Khakhar, R. M. Lueptow, and J. Ottino, Phys. Rev. Lett. **86**, 3771 (2001).
[11] P. Coussot and C. Ancey, Phys. Rev. E **59**, 4445 (1999).
[12] K. Choo, T. C. A. Molteno, and S.W. Morris, Phys. Rev. Lett. **79**, 2975 (1997).
[13] A. J. Bray, Adv. Phys. **43**, 357 (1994).
[14] J. D. Shore and J. P. Sethna, Phys. Rev. B **43**, 3782 (1991).
[15] I. S. Aranson and L. S. Tsimring, Phys. Rev. Lett. **82**, 4643 (1999).
[16] I. S. Aranson, L. S. Tsimring, and V. Vinokur, Phys. Rev. E **60**, 1975 (1999).
[17] K. M. Hill, N. Jain, and J. Ottino, Phys. Rev. E **64**, 011302 (2001).
[18] C. Chevallard, M. Nobili, and J. M. Gilli, Liq. Cryst. **28**, 179 (2001).